Tunneling in CdTe Schottky Barriers

G. H. PARKER AND C. A. MEAD
California Institute of Technology, Pasadena, California 91109
(Received 3 February, 1969)

The tunneling characteristics of metal contacts on n-CdTe have been measured. Both the forward- and reverse-bias characteristics are in good agreement with the two-band model for the energy–complex-momentum relationship. The presence of trapping states increased the magnitude of the tunneling current at low levels by providing a two-step transition. The slope of the forward-bias $\log_e J$-versus-V curves for tunneling through the intermediate states was reduced by a factor of 2.

I. INTRODUCTION

IN 1962 Lewicki and co-workers[1,2] presented a technique for determining the energy-complex-momentum relationship in insulators by studying the tunneling characteristics of Al-AlN-Mg structures. Later Padovani and Stratton[3] extended the technique to semiconductors through the use of Schottky barriers on GaAs. The study of other materials has been restricted somewhat by the problems of obtaining the high carrier concentrations necessary for the formation of narrow space-charge regions with the Schottky barriers. The present work deals with tunneling through barriers on n-type CdTe in the carrier concentration range 1.3×10^{17} to 6.0×10^{17} cm^{-3}, as compared to the 10^{18} or 10^{19} cm^{-3} used in the GaAs experiments. The low concentration reduces the magnitude of the forward-bias tunneling current to a point where it is possible to observe tunneling through the forbidden gap only near the band edge. The results are nonetheless useful in that they give a measure of the E-k dispersion relation near the band edge and hence a measure of the effective mass of the light electron or hole bands. Information about the E-k relation near midgap was obtained by measuring the reverse-bias tunneling characteristics as a function of barrier energy. The results of tunneling experiments on CdTe also indicate that the presence of trapping centers can play an important role in the tunneling process.

II. THEORY

We shall first restrict ourselves to the low-temperature J-V characteristics of thin Schottky barriers, i.e., where the primary current mechanism is the quantum-mechanical tunneling of electrons through the barrier. When the diode is under forward bias at low temperatures, the tunneling occurs from the edge of the space-charge region at the conduction band energy through the barrier into the metal. Under reverse bias the tunneling occurs from the metal to the conduction band in the semiconductor. These two cases will be treated separately because in the forward-bias case both the region of the forbidden gap and the tunneling distance are functions of voltage whereas in the reverse-bias case only the latter varies.

A. Forward J-V Characteristics

As seen in Fig. 1, the potential energy E of the barrier as measured with respect to the energy at the bottom of the conduction band in the bulk of the material is given by[3]

$$E=Nq(l-x)^2/2\epsilon, \tag{1}$$

where N is the impurity concentration in the semiconductor, q is the charge on the electron, x is the distance measured from the metal, ϵ is the permittivity of the semiconductor, and

$$l=[2\epsilon(\varphi_B-V-\xi)/Nq]^{1/2} \tag{2}$$

the width of the space-charge layer in the semiconductor. Here φ_B is the barrier energy, and ξ is the semiconductor Fermi energy.[4]

In order to calculate the tunneling current, we must assume a specific energy-momentum relationship for the electrons in the forbidden gap. The solution to Schrödinger's equation for the motion of electrons in a periodic potential using the "nearly free electron" approximation results in the following expression[5]:

$$E=\tfrac{1}{2}E_g\pm\tfrac{1}{2}(E_g^2-2\hbar^2k^2E_g/m^*)^{1/2}, \tag{3}$$

where E is the energy measured from the conduction

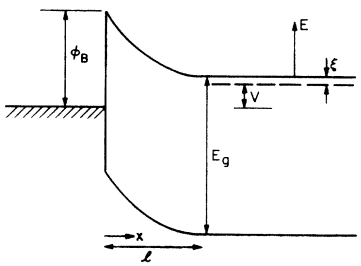

FIG. 1. Electron potential energy diagram of a Schottky barrier.

[1] G. W. Lewicki, doctoral thesis, California Institute of Technology, 1965 (unpublished)
[2] R. Stratton, G. W. Lewicki and C. A. Mead, Solid State Electron. 27, 1599 (1966).
[3] F. A. Padovani and R. Stratton, Solid State Electron. 9, 695 (1966).
[4] The notation used here is that commonly employed in semiconductor work, where the energies are given in electron volts and the electronic charge only appears explicitly in conjunction with the permittivity ϵ and the electric current.
[5] W. Franz, in *Handbuch der Physik*, edited by S. Flügge (Springer-Verlag, Berlin, 1956), Vol. XVII.

band minimum, E_g is the band gap of the semiconductor, $\hbar$ is Planck's constant, and m^* is the effective mass of the electron. k is the wave number, which is real in the conduction and valence bands, zero at the band edges, and imaginary in the forbidden gap, as shown in Fig. 2. This idealized solution requires equal values for the effective mass of the charge carriers in the conduction and valence bands. In many low-bandgap semiconductors the effective masses of the light conduction-band and the valence-band electrons are nearly equal, and this solution in fact does represent a realistic approximation.[6,7] For small values of k, i.e., near the conduction band, Eq. (3) reduces to,

$$E=\hbar^2k^2/2m^*. \tag{4}$$

The expression presented in Eq. (3) is commonly referred to as the two-band model and the expression in Eq. (4) the parabolic model. Figure 2 illustrates the E-k relationship described by the two equations.

We can now proceed to calculate the form of the tunneling current. For forward-bias voltage greater than a few kT/q, the electron current is given by

$$J=C\exp\left(-2\int_l^0 k\,dx\right), \tag{5}$$

where C is a slowly varying function of voltage and temperature.[3] In the case of large forward bias, i.e., when the applied voltage approaches the barrier potential, the tunneling occurs through only a small portion of the forbidden gap near the band edge. The parabolic model given by Eq. (4) should be valid in this region. Incorporation of the x dependence of the energy as given in Eq. (1) results in the following expression for the current:

$$J=Ce^{-s_0(\varphi_B-V-\xi)}, \tag{6}$$

where

$$\frac{d\log_e J}{dV}=s_0=\frac{2}{\hbar}\left(\frac{m^*\epsilon}{N}\right)^{1/2}.$$

Padovani and Stratton[3] have carried out a detailed calculation based on this model with which Eq. (6) is in agreement.[8]

At low forward bias the tunneling will occur through a larger portion of the forbidden gap and some deviation from the parabolic model would be expected. By repeating the calculation using the two-band model we find that

$$J=C\exp\{-\tfrac{2}{3}s_0E_g[(1\phi_B-V-\xi/E_g)^{3/2}-1]\} \tag{7}$$

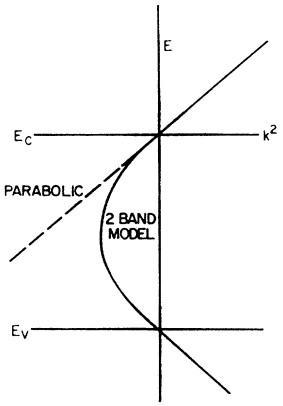

FIG. 2. Electron energy E versus wave number k.

and

$$\frac{d\log_e J}{dV}=s=s_0\left(1-\frac{\phi_B-V-\xi}{E_g}\right)^{1/2}.$$

By examining the expression for the slope of the $\log_e J$-versus-V curves we can see that the correction to the slope derived from the parabolic model is small for large forward bias in wide-bandgap materials.

B. Effect of Trapping States

We will now consider the effect of trapping levels on the forward-bias tunneling current. Since the tunneling probability is dependent on the width of the space-charge region, this probability becomes quite small as the carrier concentration in the semiconductor is reduced. However, states in the forbidden gap can act as intermediate states and increase the tunneling probability under certain conditions.[9] The situation can be analyzed in a manner analogous to that for recombination and generation through intermediate centers.[10–12]

Let us consider the following two-step process. In the forward direction, (1) the electron tunnels from the semiconductor conduction band to the state and then (2) from the state to the metal. If the concentration of states is N_t and f is the probability of occupation of the state by an electron then the number of unoccupied states is given by $N_t(1-f)$. Thus, from Fermi's "golden rule" the rates for the two processes are given by

$$R_1=C_1N_t(1-f)\exp\left(-2\int_{x_0}^{x_1}k\,dx\right)$$

and

$$R_2=C_2N_tf\exp\left(-2\int_{x_0}^{x_2}k\,dx\right), \tag{8}$$

[6] M. F. Millea, M. McColl, and C. A. Mead, Phys. Rev. **177**, 1164 (1969).
[7] G. H. Parker and C. A. Mead, Phys. Rev. Letters **21**, 605 (1968).
[8] For the case of degenerate semiconductors Conley and Mahan [J. W. Conley and G. D. Mahan, Phys. Rev. **161**, 681 (1967)] have shown that the ξ in Eq. (6) must be $\frac{3}{2}\xi$.
[9] G. H. Parker and C. A. Mead, Appl. Phys. Letters **14**, 21 (1969).
[10] A. S. Grove, *Physics and Technology of Semiconductor Devices* (John Wiley & Sons, Inc., New York, 1967).
[11] W. Shockley and W. T. Read, Phys. Rev. **87**, 835 (1952).
[12] R. N. Hall, Phys. Rev. **87**, 387 (1952).

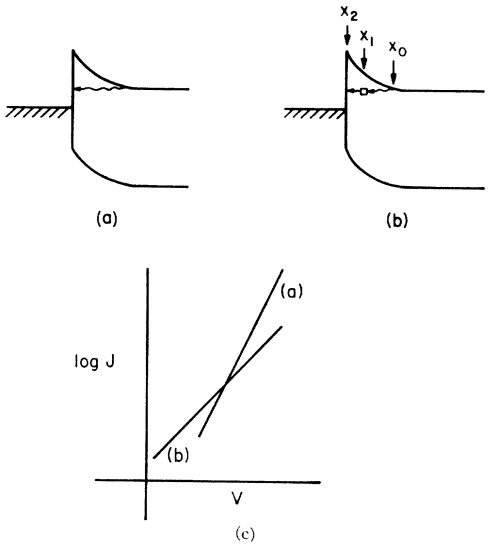

FIG. 3. Electron tunneling in the forward direction (a) with and (b) without an intermediate state. The J-V characteristics for each process are shown in (c).

where the factors C_1 and C_2 are slowly varying function of the voltage, etc. The exponentials represent the tunneling probability for each step. The limits on the integrals represent the transition steps, as shown in Fig. 3.

Under steady-state conditions, f will adjust itself until two rates are equal. Thus

$$R_1=R_2=C_1C_2N_t\exp\left[-2\left(\int_{x_0}^{x_1}kdx+\int_{x_1}^{x_2}kdx\right)\right]\Big/$$
$$\left[C_1\exp\left(-2\int_{x_0}^{x_1}kdx\right)+C_2\exp\left(-2\int_{x_1}^{x_2}kdx\right)\right]. \quad (9)$$

Equation (9) represents a peaked function which, provided C_1 and C_2 are not too different, attains its maximum value when

$$\exp\left(-2\int_{x_1}^{x_2}kdx\right)=\exp\left(-2\int_{x_0}^{x_1}kdx\right). \quad (10)$$

The rate for the completed transition will be proportional to the peak value of Eq. (9), which is just the square root of the expression for single-step tunneling.

$$R\propto\exp\left(-\int_{x_0}^{x_2}kdx\right). \quad (11)$$

The number of traps and their distribution in energy will determine the magnitude and range over which Eq. (11) is valid. If states are available in the context described above, we can repeat the procedure used in the preceding section and show that for the parabolic model the current is now of the form

$$J\propto\exp[-\tfrac{1}{2}s_0(\varphi_B-V-\xi)]. \quad (12)$$

The slope of the $\log_e J$-versus-V curves has been reduced to $\frac{1}{2}s_0$.[13] This analogous situation occurs in p-n junctions at low biases for the case of recombination via intermediate states in the space-charge region. There the states change the slope of the $\log_{10}J$-versus-V curve from q/kT to $q/2kT$.

For the present work on CdTe, we have calculated the J-V characteristics, as predicted by the two-band model with[14] $E_g=1.44$ eV, $\epsilon=10.7\epsilon_0$, and $m/m_e=0.11$. Figure 4 shows the results of the calculation plotted as $\log_e J$ versus $(\varphi-V-\xi)$.

C. Temperature Dependence

The carrier concentrations in the low 10^{17}-cm^{-3} range resulted in a slope for the $\log_e J$-versus-V curves approaching that predicted for thermionic current at 77°K. Therefore, it was necessary to include the effects of nonzero temperature in the calculation. Padovani and Stratton[3] have shown that for values of s_0 approaching q/kT the following correction is necessary:

$$\frac{d\log_e J}{dV}=s_0\tanh\left(\frac{q}{kT}\frac{1}{s_0}\right). \quad (13)$$

Because we are not far from the parabolic case the same correction can be applied to the two-band calculation. Thus, for the two-band model the slope of the J-

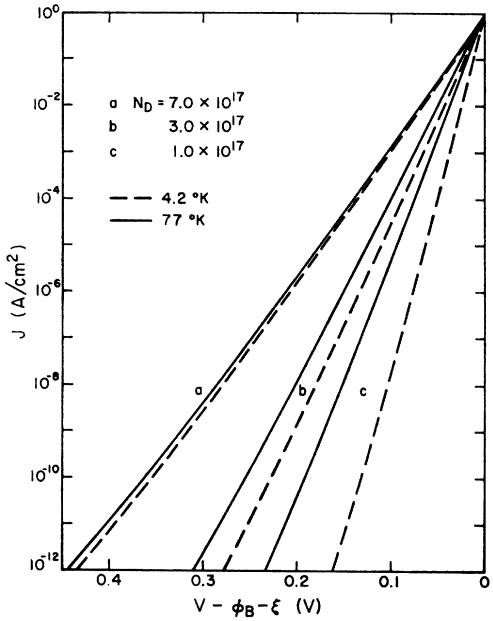

FIG. 4. Theoretical tunneling characteristics for a forward-biased Schottky barrier based on the two-band model.

[13] This result is independent of the detailed nature of the E-k relationship.

[14] Benoit a la Guillaume, *Constantes Selectionées Relatives aux Semiconducteurs* (Pergamon Press, S. A. R. L., Paris, 1961).

versus-V curve is given by

$$\frac{d\log_e J}{dV}=s\tanh\left(\frac{q}{kT}\frac{1}{s}\right), \tag{14}$$

where s is the bias voltage-dependent slope defined by Eq. (7). Figure 4 also indicates the results of this correction to the current voltage characteristics.

D. Reverse J-V Characteristics

For the reverse-bias tunneling case, the electrons tunnel primarily from near the Fermi energy in the metal to the conduction band of the semiconductor, as shown in Fig. 5. Unlike the forward-bias case, where there are no electrons available below the conduction band energy, states in the metal below the Fermi energy are filled and can contribute to the current. Like Padovani and Stratton we will make the simplifying assumption that the electric field is nearly constant over the space-charge region through which the electron tunneling takes place. Also, we will define the electron energy to be zero when it reaches the conduction band. Thus, the electron energy as a function of distance from the metal is given by

$$\mathcal{E}=\varphi_B-E_m x, \tag{15}$$

where E_m is the maximum electric field in the space-charge region.

Differentiating and substituting Eq. (1) for the maximum electric field, we find

$$d\mathcal{E}/dx=-[(2qN_D/\epsilon)(\varphi_B-\xi-V)]^{1/2} \tag{16}$$

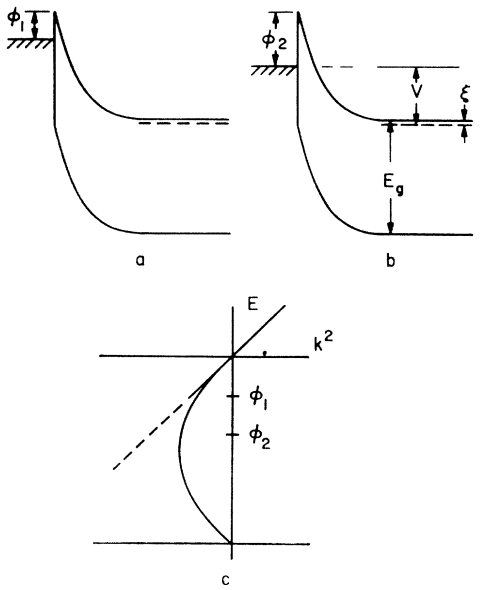

FIG. 5. Reverse-bias electron tunneling from the metal to the semiconductor for two different barrier energies, showing the different range of k involved in the two cases.

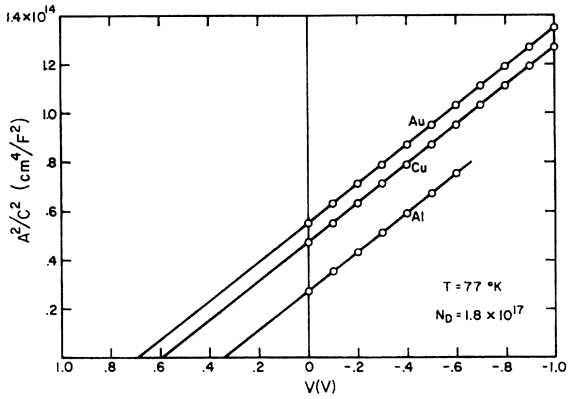

FIG. 6. Capacitance-voltage plots of Au, Cu, Al Schottky barriers on n-CdTe.

and hence the tunneling current is given by

$$J=\int_{\infty}^{\infty} f(\mathcal{E})d\mathcal{E}\exp\left[-2\int_{\varphi_B}^{0}\frac{dx}{d\mathcal{E}}k(\mathcal{E})d\mathcal{E}\right], \tag{17}$$

where $f(\mathcal{E})$ is the electron distribution in the metal. Using the supply function of Murphy and Good,[15] Eq. (17) can be written in the form

$$J=A(\varphi_B-\xi-V)\times\exp\left[2\left(\frac{\epsilon}{2qN_D}\right)^{1/2}\frac{1}{(\varphi_B-\xi-V)^{1/2}}\int_{\varphi_B}^{0}k(\mathcal{E})d\mathcal{E}\right], \tag{18}$$

where A is a slowly varying function of energy which depends on the width of the emitted electron distribution. Equation (18) is in agreement with that presented by Padovani and Stratton[3] for the low-temperature case.[16]

In the forward-bias case, it is possible to differentiate the $\log_e J$-versus-V curve and obtain the E-k relation directly, because the range of k depends upon the applied voltage. However, in reverse bias, the range of k is essentially independent of applied voltage; and, by differentiating the reverse-bias $\log_e J$-versus-V curves, one can determine only the integral over k as follows:

$$d\log_e\frac{J}{A(\varphi_B-\xi-V)}\Big/d\frac{1}{(\varphi_B-\xi-V)^{1/2}}=\left(\frac{\epsilon}{2qN_D}\right)^{1/2}2\int_{\varphi_B}^{0}k(\mathcal{E})d\mathcal{E}. \tag{19}$$

However, by varying the barrier energy φ_B one can determine the variation of the integral and compare the results with theoretical models.

[15] E. L. Murphy and R. H. Good, Jr., Phys. Rev. **102**, 1464 (1956).

[16] For the carrier concentration and in the present work, these expressions are valid at 77°K.

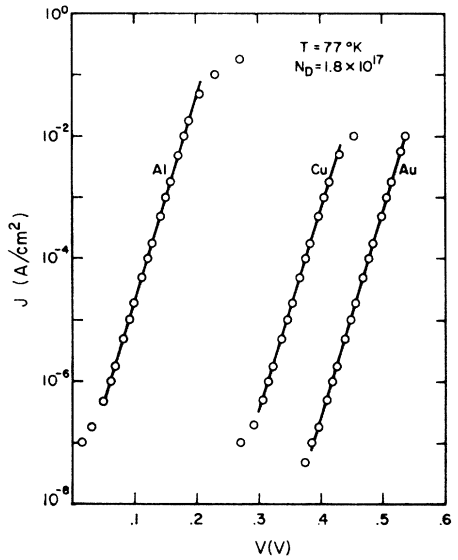

FIG. 7. Tunneling J-V characteristics of Au, Cu, Al Schottky barriers on n-CdTe, illustrating the shift due to the different barrier energies.

The image-force lowering of the barrier energy was also considered and found to decrease the integral over k only about 2% over the ranges to be considered here.

III. EXPERIMENTAL PROCEDURES

A. Sample Preparation

The CdTe crystals cleave readily on the {110} crystal planes, thereby making it possible to obtain large flat surface areas. Surfaces obtained in this manner are, of course, free of contaminants introduced by chemical cleaning procedures. It is also possible to cleave the crystal in an evaporating stream of metal in a vacuum, thereby further reducing the possibility of surface contaminants.

A special fixture was constructed to cleave the crystal in a vacuum and cover it with a metal mask. The mask was spring-loaded so that it covered the crystal immediately upon cleaving. The entire procedure was carried out in an ion-pumped vacuum system at 10^{-7} Torr.

Alternatively the CdTe may be cleaved in air and then immediately placed in a vacuum system. This technique allows selection of the best cleaved surfaces. Typical diodes were 10^{-2} cm diam. The only differences between the vacuum-cleaved and the air-cleaved samples were slightly higher values for the barrier energy on the latter (as determined from capacitance-versus-voltage measurements) which seemed to have no effect on the slope of the $\log_e J$-versus-V curves. The effect did, however, correlate with corresponding decreases in the J_0, or zero-bias intercept, obtained by extrapolation of the $\log_e J$-versus-V curves.

All of the samples used in the reverse-bias tunneling measurements were vacuum-cleaved to insure an intimate metal-semiconductor contact.

Back contact to the samples consisted of In-Ag solder which was alloyed prior to cleaving. The crystals were cut from two different CdTe ingots which subsequently led to different observed characteristics. Metals of different electronegativities were evaporated to produce a range of barrier energies. The results are given in Table I with their corresponding barrier energy as measured from capacitance voltage characteristics on the vacuum-cleaved samples. The J-V characteristics of the completed diodes were measured at room temperature both in the forward and reverse directions. Also, the carrier concentration and diffusion potential were determined from (capacitance)$^{-2}$-versus-voltage plots. The diodes were then immersed in liquid nitrogen and the measurements repeated. A special probe assembly was constructed to permit measurements at 4.2°K by lowering the sample into a storage Dewar filled with liquid helium. The slope of the (capacitance)$^{-2}$-versus-voltage curve for any given sample remained unchanged (within 5%) at all three temperatures.

B. Forward J-V Characteristics

The room-temperature J-V characteristics followed the usual diode equation:

$$J = J_0(e^{qV/nkT} - 1), \tag{20}$$

where the parameter n took on a value of 1.1.[17] The use

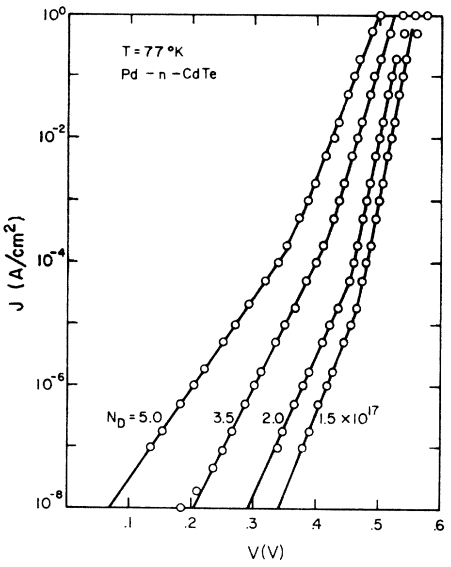

FIG. 8. Forward-bias J-V characteristics of Pd Schottky barriers on n-CdTe samples of several carrier concentrations. The upper slopes correspond to the simple tunneling theory [Eq. (13)] while the lower slopes correspond to tunneling through an intermediate state [Eq. (12)].

[17] M. M. Atalla and R. W. Soshea, Scientific Report No. 1, 1962, Contract No. Nr AF 19(628)-1637 hpa.

of several different metals for the Schottky barriers produced a range of barrier energies which permitted the consistency of the results to be checked. Figure 6 shows capacitance-voltage data on material of the same carrier concentration for three metals. The forward $\log_e J$-V characteristics taken at 77°K are illustrated in Fig. 7 and have the same slope but are displayed by exactly the difference in barrier energies, as expected from Fig. 6. The slope of these curves remained unchanged at 4.2°K, thereby giving assurance that the observed current is indeed the result of electron tunneling through the barrier. A selection of samples cut from different portions of an ingot of CdTe provided a range of carrier concentrations. According to Eq. (6), variations in carrier concentration should be reflected in the slope of the low-temperature $\log_e J$-versus-V curves. Figure 8 illustrates the tunneling characteristics of Schottky barriers of the same barrier energy for several carrier-concentration levels in the CdTe. The $\log_e J$-versus-V curves exhibit two distinct regimes, whose slopes differ by a factor of 2. The upper regime is in agreement with the calculation based on the parabolic model given by Eq. (6), whereas the lower regime is attributable to tunneling of electrons via an intermediate state [Eq. (12)].

A second group of diodes was similarly fabricated from a different ingot of CdTe and the above procedure repeated. The J-V characteristics as illustrated in Fig 9 now show only a single regime, which correlates with the intermediate-state tunneling calculation [Eq. (12)]. These results were not surprising in view of the fact that this particular ingot was prepared in such a manner that it was expected to have a high density of shallow trapping centers.

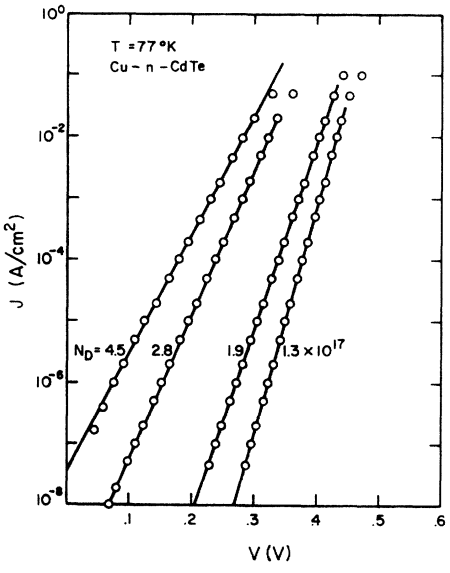

FIG. 9. Tunneling J-V characteristics of Cu Schottky barriers on n-CdTe samples of different carrier concentration.

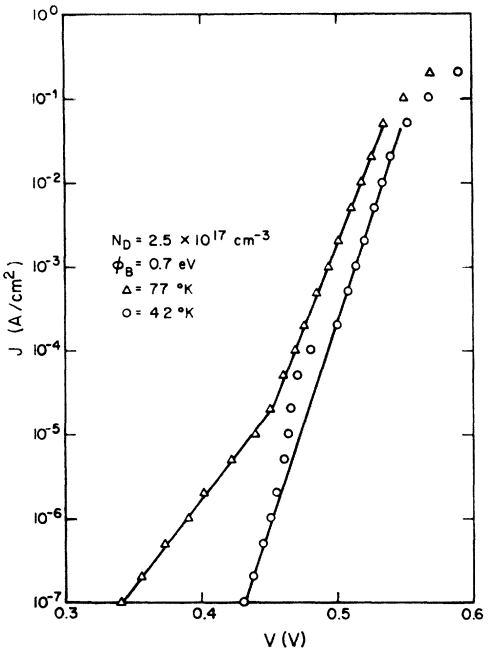

FIG. 10. Tunneling J-V characteristics showing the effect of traps at 77 and at 4.2°K.

The wide range of energy over which tunneling occurred via intermediate states can be attributed to thermal broadening of the peak of Eq. (9) at 77°K. The diode J-V characteristics began to exhibit structure when the samples were cooled to 4.2°K, thus confirming that trapping states are responsible for the observed behavior. Figure 10 shows a typical characteristic taken at 77 and 4.2°K.

The dual slope behavior which was observed in these tunneling measurements is analogous to that observed in the forward J-V characteristics of p-n junction diodes in silicon and gallium arsenide.[10] There the dual slope is attributable to the recombination in the space-charge region at small applied bias and to minority carrier injection at larger forward bias.

We believe that the effect of traps on tunneling have not been identified before because in most tunneling measurements large carrier concentrations are used to obtain high tunneling probabilities. Thus, the magnitude of the single tunneling step current would be greater than that expected for tunneling through intermediate states. However, in barriers on low carrier-concentration materials excess currents are frequently observed and have not been understood.[18] In these later cases tunneling through traps may be involved.

The limited range of forward-bias voltage (or energy) over which the tunneling current is unambiguously observed in the present diodes does not enable us to distinguish between the parabolic and the two-band

[18] F. A. Padovani, in *Semiconductors and Semimetals—Physics of III-V Compounds* (Academic Press Inc., New York, 1969).

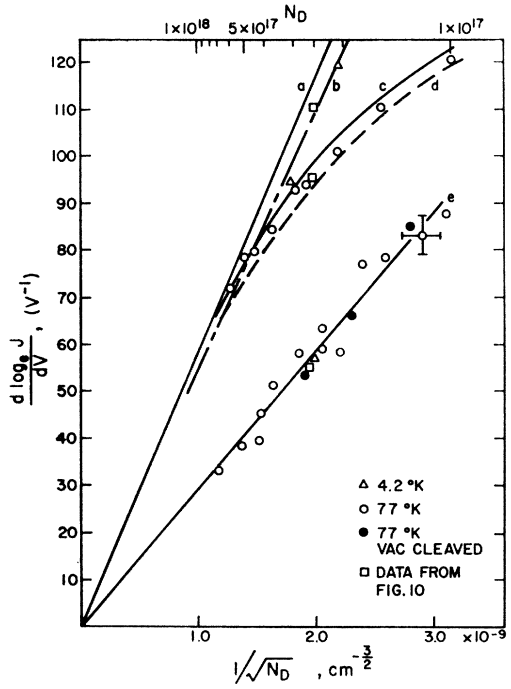

FIG. 11. Slope of the forward-bias $\log_e J$-V tunneling curves as a function of carrier concentration. Experimental points are taken from curves such as Figs. 7–9. (a) Theoretical curve based on parabolic band model at 4.2°K, (b) two band model at 4.2°K and evaluated at $(\varphi_B - V - \xi) = 0.150$ V, (c) parabolic model at 77°K, (d) two-band model at 77°K, $\varphi - V - \xi = 0.150$ V, (e) parabolic model for tunneling via an intermediate state at 77°K. Theoretical curves were computed from the published value (Ref. 11) of the effective mass and contain no adjustable parameters.

E-k dispersion relation. Thus, we have taken the tunneling $\log_e J$-V curves as straight lines, which is characteristic of the parabolic model. The slopes of these straight lines are presented in Fig. 11 as a function of carrier concentration for the diodes exhibiting both one and two regimes. Curve A represents the computed value s_0 as a function of carrier concentration and is thus the slope of the $\log_e J$-versus-V curves for the parabolic model, neglecting thermal effects. Curve B represents the slope as computed from the two-band model and evaluated at $\varphi_B - \xi - V = 0.150$ V; a typical bias condition at which the slope would be measured.

TABLE I. Barrier energies as measured from capacitance-voltage characteristics for metals of different electronegativities.

Metal	V_D(Cap) (eV)
Al	0.35±0.02
Mg	0.40
In	0.50
Ni	0.53
Cu	0.57
Ag	0.65
Pd	0.65
Au	0.69

Curves C and D have included the temperature dependence at 77°K for the two models as expressed in Eqs. (13) and (14). Curve E shows the case of tunneling via an intermediate state and is plotted as $\frac{1}{2}s_0$ versus $1/N^{1/2}$. Good agreement is obtained in all cases.

The possibility of an edge effect contribution to the observed J-V characteristics was investigated in two ways. First, dots of two different areas were evaporated onto two opposing freshly cleaved crystal faces. The current at any given voltage was directly proportional to the area while the slope of the $\log_e$J-versus-V curve remained the same. Second, 0.02-cm-diam dots of aluminum were evaporated onto a cleaved crystal. Then, after measuring the J-V characteristics, 0.04-cm-diam dots of gold were evaporated, centered over the aluminum dots. The J-V characteristics of these new structures showed no change in the range of interest. Since the Al-CdTe barrier energy is 0.35 V and the Au-CdTe barrier energy is 0.69 V, the current to be expected from a gold barrier is many orders of magnitude below that observed on the aluminum barrier. Thus, we can conclude that the perimeter of the metal dots does not make a noticeable contribution to the J-V characteristics as far as we are concerned with them in this discussion.

C. Reverse J-V Characteristics

In the case of the forward-bias characteristics, a change in barrier energy merely moved the $\log_e J$-versus-V curves horizontally on the voltage axis. However, under reverse bias, in addition to being displaced horizontally, the slope also changes. Figure 12 shows four $\log_e J$-V curves for diodes of different barrier energies. From Eq. (19) we see that if we plot

$$\log_e[J/(\varphi_B - \xi - V)] \text{ versus } (\varphi_B - \xi - V)^{-1/2}.$$

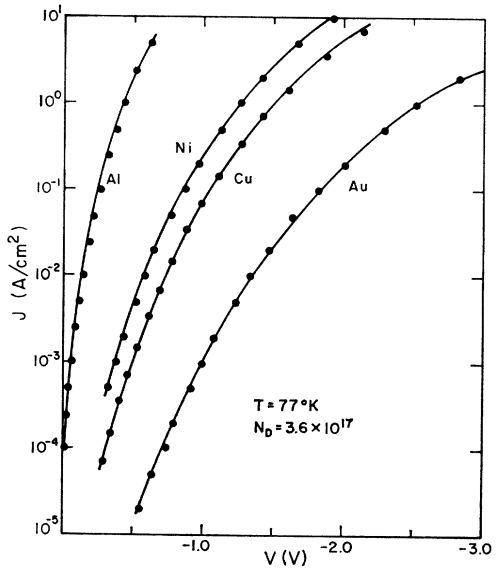

FIG. 12. Reverse-bias tunneling characteristics of four Schottky barriers of different barrier energies on n-CdTe.

The result should be a straight line. The slope of curves will then give a value for the integral of k over the energy range from the barrier energy to the conduction band. Data taken from Fig. 12 have been replotted in this manner in Fig. 13. Figure 14 then shows the integral of k versus barrier energy inferred from the slopes of those curves. We have plotted for comparison the theoretical values for the parabolic and two-band model with $N=3.6\times10^{17}/\text{cm}^3$. The experimental points are also normalized to this value of carrier concentration. This data clearly indicates that the E-k dispersion relation in the forbidden gap in CdTe is in good agreement with the two-band model. Several samples were also measured at 4.2°K, and the results were in agreement with those obtained at 77°K.

IV. CONCLUSION

We have observed electron tunneling current in metal-n-CdTe junctions. The observed slope of the large forward-bias $\log_e J$-V characteristics was in good agreement with that calculated using the accepted value of 0.11 for the electron effective mass. The influence of trapping states on the forward characteristics has been shown to reduce the slope of the $\log_e J$-V curves by a factor of 2 under the proper conditions. We have also demonstrated a new technique which utilizes the reverse-bias tunneling characteristics to determine the electron wave vector, and thereby shown that in CdTe the E-k dispersion relation through the forbidden gap corresponds to that predicted by the two-band model. The techniques presented here have potential applications in determining carrier concentration very near the surface of a semiconductor and the effective mass of charge carriers in the direction of current flow. The two-step tunneling process which was discussed offers a potentially powerful tool for determining the distribution of traps in the forbidden gap. Finally, the reverse-bias technique has been shown to give excellent results and is especially applicable to low carrier-concentration material.

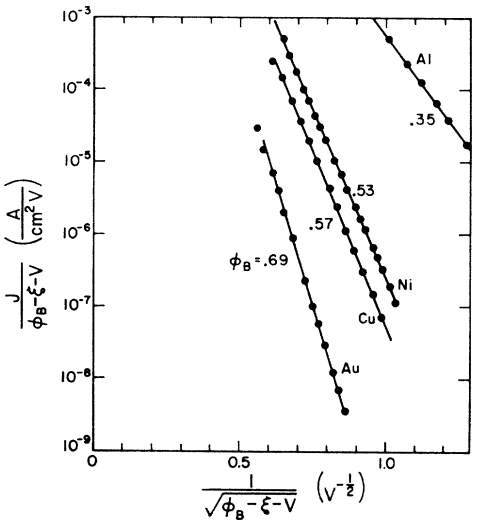

FIG. 13. Fowler-Nordheim-type plot of the data of Fig. 12 showing systematic variation of slope with barrier energy.

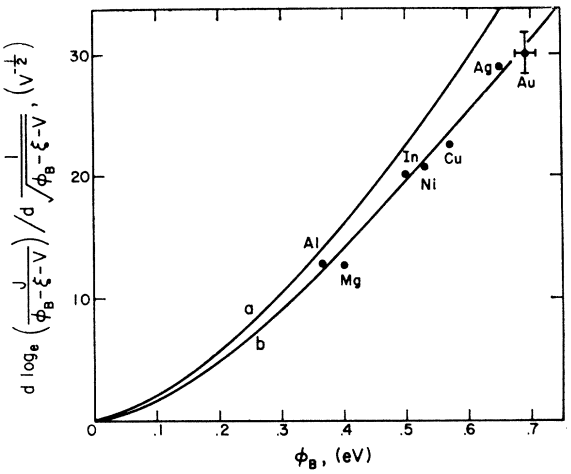

FIG. 14. Plot of the integral of k from the Fermi energy in the metal to the semiconductor conduction band for (a) the parabolic model and (b) the two-band model as a function of barrier energy. The experimental points are those obtained from the slopes of the curves like those of Fig. 13.

ACKNOWLEDGMENTS

We wish to thank L. van Atta, G. Picus, and N. Kyle of the Hughes Research Laboratories for supplying the CdTe used in this work. The work was supported in part by the Office of Naval Research.